Accretion Dynamics and Pulse Profile Asymmetry in X-ray Pulsars with Misaligned Neutron Star Rotation

Vedant Ganesh[†]

Project advisor: Alexander Mushtukov[‡]

Abstract. The dynamics of accretion in X-ray pulsars (XRPs) are shaped by the surrounding magnetic field. Charged material in the accretion disk impacts the magnetosphere and is constrained to the magnetic field lines due to the strength of the field. The particles' dynamics are then influenced by extremely large gravitational forces due to high density and proximity, and centrifugal forces due to the corotation of the XRP magnetosphere. At higher mass accretion rates, radiative force appears which heavily influences the magnetic field flow. Accretion flows follow the magnetic field lines to impact the neutron star in a small region near the magnetic poles. We construct a numerical model to help determine the dynamics of accretion flow under these conditions and investigate its effects on the mass accretion rate and pulse profile of XRPs, assuming that the magnetic field is dominated by the dipole geometry. We show that variability in mass accretion rate, and hence pulse profile asymmetry, can be due to the misalignment between the accretion plane normal, rotational, and dipole axes, and we investigate the effects of each angle on pulse profile asymmetry.

1. Introduction. Neutron stars (NSs) are extremely dense stellar remnants that form after the collapse and supernova explosion of stars with mass $\geq 10\,\mathrm{M}_\odot$, where hydrostatic equilibrium is due to the balance between gravity and the pressure gradient of degenerate neutrons and other strongly interacting massive particles. Some NSs are highly anisotropic sources emitting with short peak wavelengths and at high, occasionally super-Eddington, luminosities, and their spin periods vary widely, ranging from $10^3\,\mathrm{s}$ to $10^{-3}\,\mathrm{s}$.

X-ray pulsars (XRPs, see, e.g., [8]) are strongly-magnetized accreting NSs present in binary systems that orbit their companion closely. The companion star provides a significant amount of mass that can be accreted onto the NS in XRP, leading to high mass accretion rates and high luminosity [6].We estimate the luminosity of the XRP to be equal to the kinetic energy delivered to the NS surface using the following expression, where v_{ff} is the freefall velocity of material at the NS surface and $\dot{M}$ is the mass accretion rate:

$$L \approx \frac{1}{2}\dot{M}v_{\mathrm{ff}}^2 \approx \frac{GM\dot{M}}{r} \tag{1.1}$$

The dynamics of XRP accretion are dominated by gravitational force, centrifugal force, radiative force, and the presence of the strong magnetic fields in excess of 10^{12} G. Due to the plasma nature of the accreting material, most accreting particles are charged and so experience extreme Lorentzian forces which constrain their motion to magnetic field lines. The high density of XRPs (masses in excess of $1.4\,\mathrm{M}_\odot$ packed into an object with radius $\sim 10^6\,\mathrm{cm}$) cause accreting material to accelerate rapidly towards the XRP surface due to strong gravitational attraction. Corotation of the magnetic field lines with a relatively low spin period (ranging from $100\,\mathrm{s}$ to $0.1\,\mathrm{s}$) causes accretion flow constrained to move along magnetic field lines to

[†]Tanglin Trust School, Singapore (vedant.ganesh@tts.edu.sg).
[‡]University of Oxford alexander.mushtukov@physics.ox.ac.uk

experience a centrifugal force, which also influences accretion dynamics significantly. Finally, at high accretion rates $\geq 10^{17}\,\mathrm{g\,s^{-1}}$, radiative scattering in the magnetospheric flows leads to significant momentum transfer and thus the appearance of non-negligible radiative force. The

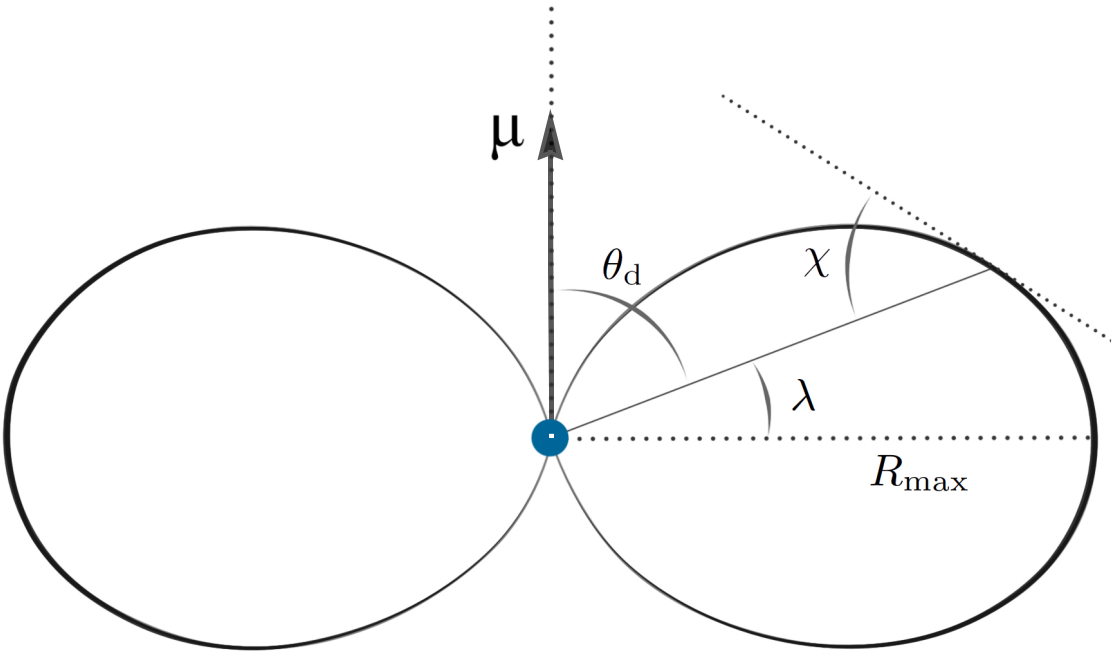

Figure 1. *The schematic geometry of dipole magnetic field line, where $R_{\max}$ is the linear scale describing magnetic field line, λ (θ_d) is the latitude (co-latitude) of a point, and χ is the angle between the position point and the tangent line to the field line. The figure is taken from [9].*

magnetic field of an XRP also directs accretion flow towards the poles of the star, as shown in Figure 1. This leads to a large variance in NS surface temperatures with intense "hot spots" in very small areas near the poles, which causes extreme anisotropy in XRP radiation and the characteristic pulsations of an XRP.

At certain combinations of low rotational periods and low mass accretion rates, a centrifugal barrier appears in regions close to the magnetospheric equator where centrifugal force is greater than gravitational force along magnetic field lines. This phenomenon is the "propeller" mode of accretion, which has been described in [12].

Because of the strong anisotropy of NS radiation, alongside their rotation, the observed flux of NSs varies significantly with time in a periodic fashion due to NS alignment relative to the observer. It is expected that with low mass injection rates from the companion star and aligned rotational axes and magnetic moment, the mass accretion rate at the NS surface is constant, leading to constant luminosity and hence a symmetric pulse profile. However, the dynamics of magnetospheric matter flows in cases where the magnetic axis is inclined relative to the spin axis and accretion disc plane have not been widely studied. Some relevant research has been undertaken (e.g. in [10] and [11]), but these works focus predominantly

on relatively small magnetospheres prevalent in accreting millisecond pulsars. In those cases, pulse profile asymmetry arises primarily from complex spot morphologies. However, similar studies of inclined rotators in X-ray pulsars are, to our knowledge, absent. In this paper, we investigate XRP accretion with misaligned dipole, rotational, and accretion disk plane axes, and its effect on the pulse profile of the XRP.

The paper is organized as follows. The relevant physics is theoretically treated in section 2, our numerical method is in section 3, and the simulation results are in section 4.

2. Physical model. We assume that the geometry of XRPs deviates negligibly from a sphere (i.e. the rotation is sufficiently slow to negligibly impact NS shape). We also assume corotation of the NS magnetosphere with the NS, and that the geometry of the NS magnetosphere is dominated by a dipole component. For calculations of the radiative force, we assume that radiation emitted from regions other than the poles is negligible.

2.1. Geometry of Accretion Flow. In this paper, we consider accretion flow starting at the accretion disk. We assume that accreting material enters the system from a thin flat surface. We also assume that NS magnetic field lines, along which accretion flows move, have a dipole geometry. In this case, the magnetic field line is given by the following expression, where λ represents the latitude:

$$R = R_m \cos^2 \lambda \tag{2.1}$$

We define R_m to be the maximum radius of the magnetic field line in units of cm. An estimate for this quantity is given by [2] as:

$$R_m \approx 1.8 \times 10^8 \, \Lambda \, B_{12}^{4/7} \dot{M}_{17}^{-2/7} m^{-1/7} R_6^{12/7} \tag{2.2}$$

Where Λ is a parameter between 0 and 1, B_{12} is the magnetic field strength in units of 10^{12} G, $\dot{M}_{17}$ is the mass accretion rate in units of $10^{17}\,\mathrm{g\,s^{-1}}$, m is the mass of an NS in solar masses, and R_6 is the NS radius in units of 10^6 cm (see Figure 1).We estimate the magnetic field line radius in our simulations to be 10^8 cm, and the NS radius to be 10^6 cm. The magnetic field lines extend from R_m at the magnetospheric equator to the point where $R = R_{\mathrm{NS}}$ near the poles.

Due to the strong magnetic fields of $B \geq 10^8$ G within the magnetosphere of an NS and the high ionization of accreting particles, we can constrain the motion of the particles to being along magnetic field lines. The rate of change of arc length against latitude is given by the following equation:

$$\frac{\mathrm{d}s}{\mathrm{d}\lambda} = R_m \cos\lambda \sqrt{1 + 3\sin^2\lambda} \tag{2.3}$$

Integrating the above, we obtain:

$$s\,(\lambda) = \frac{R_m}{6}\left(\sqrt{3}\,\mathrm{arcsinh}\left(\sqrt{3}\sin\lambda\right) + 3\,\sin\lambda\,\sqrt{1+3\sin^2\lambda}\right) \tag{2.4}$$

In the case of an NS with a magnetic moment not aligned with the normal to the accretion plane, the latitude λ_0 of the accretion disk and its intersection with the magnetosphere is

nonzero and varies with azimuthal angle φ. Assuming the rotational axis is aligned with the magnetic moment, the latitude of the disk plane as a function of azimuthal angle φ and the inclination of the magnetic moment from the accretion disk normal β is given by the following expression:

$$\lambda_0 = \arctan\left(\frac{\sin\varphi}{\tan\beta}\right) \tag{2.5}$$

In this paper, we further consider XRPs with misaligned magnetic dipole, rotational, and accretion plane normal axes, in which case the initial latitude of particle injection becomes both time- and phase-dependent. We find the coordinates of the disk normal to be as follows (see section 6):

$$\mathbf{n} = \begin{bmatrix} \sin\beta\sin\omega t \\ -\left(\cos\beta\sin\alpha + \cos\alpha\sin\beta\cos\omega t\right) \\ \cos\beta\cos\alpha - \sin\beta\sin\alpha\cos\omega t \end{bmatrix} \tag{2.6}$$

We then consider λ to be the slope angle between the xy-plane and the disk plane, finding the equation for the starting latitude λ_0 of particles as a function of the azimuthal angle φ and rotational phase ωt in the magnetospheric frame of reference. The expression is as follows, where n_x is the x-component of the disc normal $\mathbf{n}$ as given in (2.6):

$$\lambda_0\left(\varphi, \omega t\right) = \arcsin\left(n_x\cos\varphi + n_y\sin\varphi\right) \tag{2.7}$$

2.2. Consideration of Forces.

2.2.1. Gravitation. The gravitational force on the object is given by:

$$a_g = -\frac{GM}{|\mathbf{r}|^3}\mathbf{r}\cdot\hat{n}_B \tag{2.8}$$

where $\mathbf{r}$ is the radius vector from the NS barycentre to the object, $\cdot$ denotes the dot product, $\hat{n_B}$ denotes the dimensionless unit vector along magnetic field lines, M is the mass of the pulsar, and $G = 6.67\times10^{-8}\mathrm{dyn\,cm^2\,g^{-2}}$ is the universal gravitational constant. Here, the sign convention is chosen such that a negative (positive) sign of a_g indicates decreasing (increasing) λ.

2.2.2. Centrifugal force. Because of the rapid rotation and large maximum radius of the NS magnetosphere, the centrifugal force becomes significant in considering the kinematics of magnetospheric flows. We calculate the centrifugal acceleration using (2.9), where $\boldsymbol{\omega}$ is the angular velocity vector of the NS rotation, $\mathbf{r}$ is the radius vector of the particle, and $\hat{n}_B$ is the unit vector along magnetic field lines.

$$a_c = -\left(\boldsymbol{\omega}\times\left(\boldsymbol{\omega}\times\mathbf{r}\right)\right)\cdot\hat{n}_B \tag{2.9}$$

We take the vector projection onto the magnetic field l ine o nce a gain d ue t o t he applied constraint. Therefore, where radiative effects are negligible, we take the total acceleration

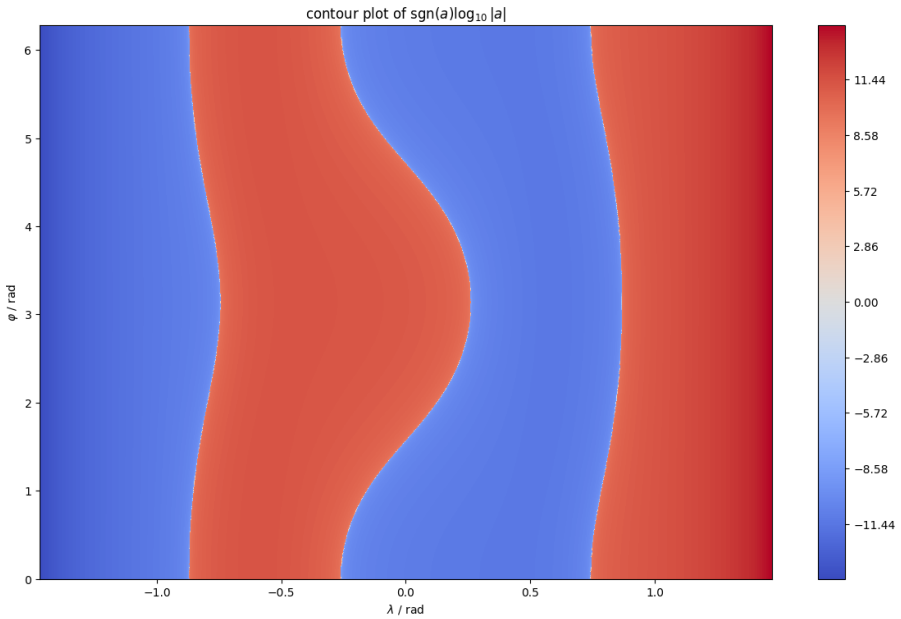

Figure 2. *The dependence of acceleration on latitude (λ) and azimuthal angle (φ), neglecting radiative force. Forces calculated with parameters $M = 1.4\,\mathrm{M}_\odot$, $R_m = 10^8\,\mathrm{cm}$, and $\beta = 1\,\mathrm{rad}$. Using $\alpha \neq 0\,\mathrm{rad}$ results in a time-varying acceleration for each point.*

$a = a_g + a_c$ along magnetic field lines to find the acceleration of a particle at a position $\mathbf{r}$. An example plot of acceleration against latitude and azimuthal angle is given in Figure 2. The misalignment of the XRP rotation axis with the other axes creates a dependence of acceleration against azimuthal angle (exaggerated here for visual clarity). This dependence also varies with time where the rotational and dipole axes are misaligned.

2.2.3. Effects of Radiative Force. At high mass accretion rates past $10^{17}\,\mathrm{g\,s^{-1}}$, radiative force arises in NS accretion dynamics. Radiative force is caused by the energy of accreting particles heating hot spots on the NS surface, leading to emission at the poles. Due to extremely high temperatures in XRP hot spots, the large majority of emission from XRPs is in the hard X-ray range. This radiation follows a curved trajectory through spacetime, and later impacts the magnetosphere, scattering within it and thus transferring momentum to accreting particles. At high mass accretion rates, there is a considerable energy flux from the NS surface and thus a non-negligible radiative momentum transfer to particles in the magnetosphere.

We assume that the total energy emitted by the NS in a time interval t is given by (2.10), i.e. the sum of the relativistic kinetic energies of the i particles that impact the NS surface during the time interval t. In this expression, γ_i denotes the Lorentz factor of the i-th particle.

Typically for rates around $10^{16}\,\mathrm{g\,s^{-1}}$, NS luminosity will be around $10^{37}\,\mathrm{erg\,s^{-1}}$. We consider this equation rather than (1.1) as (1.1) neglects changes in velocity owing to centrifugal force.

$$E = \sum_i (\gamma_i - 1)\, m_i c^2 \tag{2.10}$$

Currently, the distribution of radiation from the NS surface is unknown, so we model this with the distribution

$$\Phi_e \propto a \cos\alpha \tag{2.11}$$

where $\alpha \in [-\frac{\pi}{2}, \frac{\pi}{2}]$ is the angle between the normal to the NS surface at the point. The simulation parameter $a \in [0, 1]$ determines the emission pattern of the NS, with $a = 0$ corresponding to equal intensity of emission regardless of the obliquity of emission and $a = 1$ being a Lambertian surface.

We model the magnetospheric flow as geometrically and optically thin, and thus model the scattering processes in the magnetosphere as being dominated by the first scattering only, and that the effect of subsequent photon scattering on momentum transfer is negligible.

Using this model, the radiative force F depends on the photonic impact angle γ, the optical thickness τ estimated using (2.13), and the luminosity $\frac{dE}{dt}$ of the XRP poles. The radiative force is given by the following equation:

$$F = \frac{\mathrm{d}p}{\mathrm{d}t} = \frac{\mathrm{d}E}{dt}\,\frac{1}{c}\left(1 - \exp\left(-\frac{\tau}{\sin\gamma}\right)\right)\cos\gamma \tag{2.12}$$

We estimate τ, the unitless optical thickness, using the following expression:

$$\tau = \mathrm{d}A\Sigma\frac{1}{m_p} \tag{2.13}$$

Here, $\mathrm{d}A$ is the infinitesimal area of the magnetospheric surface (units of cm^2), Σ is the local surface density in units of $\mathrm{g\,cm^{-2}}$, and m_p is the mass of a proton. We assume that the accreting plasma has negligible metallicity, so we approximate it as 100% ^{1}H (ionised protium). We include a plot of the photonic impact angle γ against magnetospheric latitude λ:

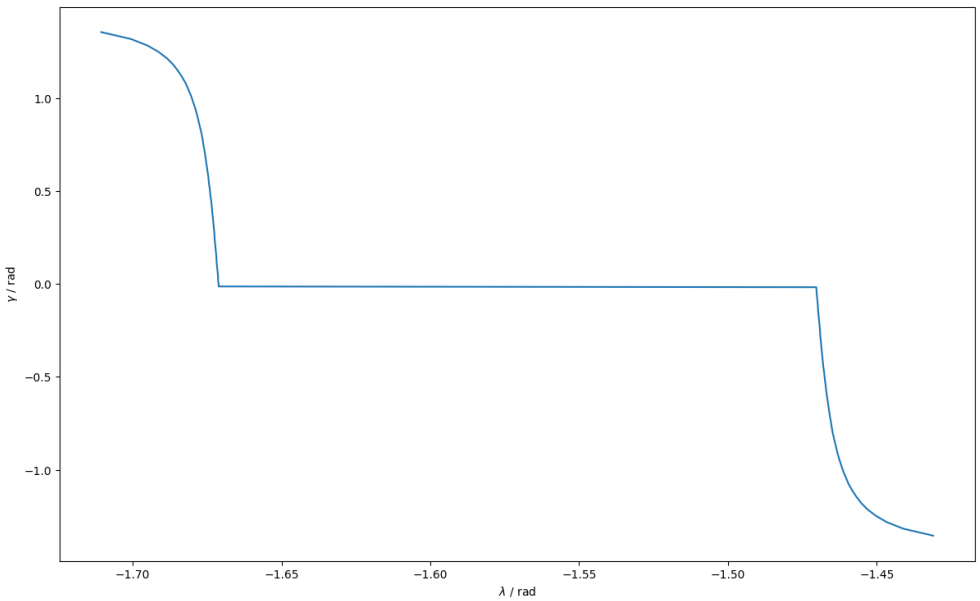

Figure 3. *The photonic impact angle, γ, against the latitude λ at which the photon impacts the magnetosphere. Calculated with $M = 1.4\,\mathrm{M}_\odot$, $R_m = 10^8\,\mathrm{cm}$, and $R_{\mathrm{NS}} = 10^6\,\mathrm{cm}$. In this model all photons were assumed to originate at the magnetic pole.*

Since this model considers only the first photon scattering, the results apply only to accretion regimes with optically and geometrically thin accretion flows (i.e. $\dot{M} \leq 2 \times 10^{18}\,\mathrm{g\,s^{-1}}$). Additional scatterings would increase the radiative force on the particles, potentially influencing the magnetospheric flows, as discussed in [1]. This would however require much more advanced numerical simulations that are beyond the scope of this publication.

2.3. Gravitational lensing. Owing to the small radius and the large mass of the NS [8], there is significant gravitational lensing of light close to the surface of the NS, especially in photons emitted at oblique angles (See Figure 4). The lensing effect leads to significant differences in both the impact angle (and hence momentum transfer to the accretion flow) and the distribution of photon flux in the magnetosphere.

To find light-like geodesics, we assume that the rotation of the NS is negligible so that the Schwarzschild solution can be used. Though the Schwarzschild solution uses (ct, r, θ, ϕ) coordinates, we can describe light paths in (r, λ) coordinates without loss of generality due to the rotational symmetry of the problem. In these coordinates:

$$u'' = 3u^2 - u \tag{2.14}$$

$$u_0' = \frac{-u_0}{\tan(\alpha_\gamma - \lambda)} \tag{2.15}$$

where:

$$u = \frac{GM}{c^2 r} = \frac{0.5 r_s}{r} \tag{2.16}$$

is the coordinate transformation applied to simplify the calculation; u'' denotes the second derivative of u with respect to λ; and α_γ is the obliquity of emission (i.e. the angle between the initial emission angle and the normal to the surface). See Figure 4.

We then calculate the photon trajectory in (r, θ) coordinates. Combining these two equations and the arc-tangent relation, we can compute the angle η between the light-ray's final travel and the direction of the photon flow. In this case, $\cos\eta$ gives the projection of photon motion onto the magnetospheric flow, enabling calculations of radiative force applying constraints of magnetic field lines. These were pre-calculated, and (2.12) was simplified for each path to

$$F = k\frac{\mathrm{d}E}{dt}$$

, where $\frac{\mathrm{d}E}{dt}$ is the energy flux emitted along that particular light ray trajectory, and k is a constant for each path.

3. Numerical Model. Our numerical simulations relied on starting particles at uniform, random locations at the accretion disk boundary and using the leapfrog integrator to numerically approximate the trajectory of accreting particles. This integrator was chosen because of its simplicity and its explicitly energy-conserving nature. The convergence and stability of the integrator were tested by varying the minimum timestep and ensuring reproducibility of the results. We numerically solved the gravitational lensing equation using a second-order integrator, recording the end-points and final angles of each light path. The steps are as follows:

1. Calculate the position vector $\mathbf{r_n}$ and the vector along magnetic field lines $\mathbf{n_B}_n$, given the latitude λ and the azimuthal angle φ of the particle.
2. Calculate a as the sum of $a_g(t_n)$, $a_{cen}(t_n)$, and $a_{rad}(t_n)$ using (2.8), (2.9) and (2.12).
3. Calculate the displacement ds of the particle using the formula $ds_n = v_n\,dt + \frac{1}{2}a_n\,dt^2$.
4. Calculate the new latitude using the equation for $\frac{d\lambda}{ds}$.
5. Calculate the new velocity $v_{n+1} = v_n + a_n\,dt$
6. Find the particles that have reached the NS surface, and remove them from the simulation - thus, calculate the mass accretion rate with

$$\dot{M}_n = \frac{\sum_i m_i}{\Delta t}$$

   where i is an index over the particles that have reached the XRP surface in the previous time increment.
7. Use (2.10) to find the luminosity at the next timestep. This equation is preferred over (1.1) as the expression of relativistic kinetic energy accounts for the centrifugal force where Eqn. (1.1) does not.
8. compute the next timestep Δt using the heuristic $\Delta t = \min(\frac{\Delta s}{5v})$
9. compute the next time $t_{n+1} = t_n + \Delta t$
10. Repeat from step 1.

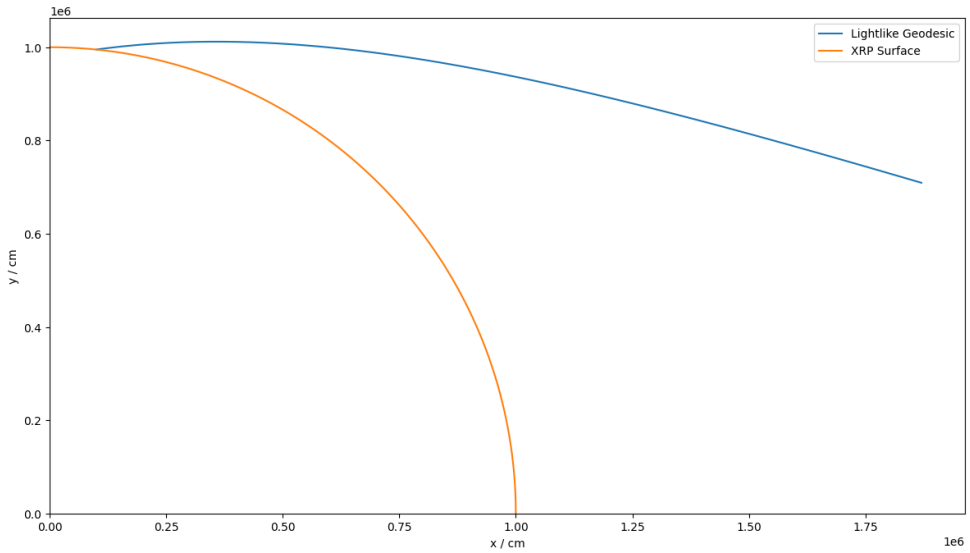

Figure 4. *An example photon trajectory showing obvious light bending in the vicinity of the NS calculated with the above ODE and the RK4 method. Parameters:* $M = 1.4\,\mathrm{M}_\odot$, $R_m = 10^8\,\mathrm{cm}$, $R_{\mathrm{NS}} = 10^6\,\mathrm{cm}$, $\lambda_0 = \arccos\left(\sqrt{\frac{R_{\mathrm{NS}}}{R_m}}\right) \approx 84.26^\circ$, *and* $\alpha_\gamma = 1.5\,\mathrm{rad}$. *The expression for* λ_0 *represents the latitude where magnetospheric flows impact the NS surface.*

4. Results. Figure 5 illustrates the mass accretion rate onto the NS surface for two cases of spin periods: $P_{\mathrm{spin}} = 1\,\mathrm{s}$ (red line) and $P_{\mathrm{spin}} = 2\,\mathrm{s}$ (black line), with a fixed misalignment angle of $\beta = 5^\circ$ between the normal to the accretion disc plane and the NS rotational axis. The simulations were performed for a low mass accretion rate of $\dot{M} = 10^{15}\,\mathrm{g\,s^{-1}}$, allowing radiative forces to be neglected. The NS parameters were fixed at $M = 1.4\,\mathrm{M}_\odot$ and $R = 1 \times 10^6\,\mathrm{cm}$. The results demonstrate that the amplitude of mass accretion rate variability at the NS surface depends strongly on the NS spin period, in that the variability amplitude decreases as the spin period increases. This behavior can be attributed to the interplay between the gravitational and centrifugal forces acting on matter along the magnetic field lines, which is influenced by the rotational period of the NS. Importantly, the average mass accretion rate at the NS surface over time remains equal to the mass accretion rate at the inner disc radius, which was assumed to be constant in these simulations. This highlights that the variability does not affect the overall accretion efficiency but introduces periodic fluctuations in the rate at which material reaches the NS surface. These findings clearly show the role of NS spin period, and hence centrifugal force, in creating periodic variations in mass accretion rate and hence asymmetries in the pulse profile of XRPs.

Figure 6 presents the mass accretion rate onto the NS surface as a function of time,

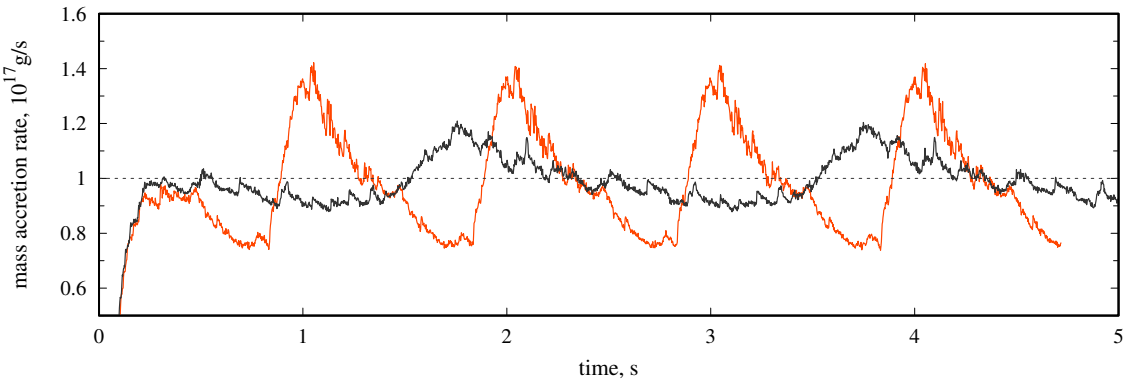

Figure 5. *Mass accretion rate onto NS surface for the case of NS spin period* 1 s *(red line) and* 2 s *(black line). The angle between the normal to accretion disc plane and NS rotational axis is fixed at* $\beta = 5°$. *Mass accretion rate was taken to be small* ($\dot{M} = 10^{15}\,\mathrm{g\,s^{-1}}$) *so radiative force could be ignored. Parameters:* $M = 1.4\,\mathrm{M}_\odot$, $R_{\rm NS} = 10^6$ cm.

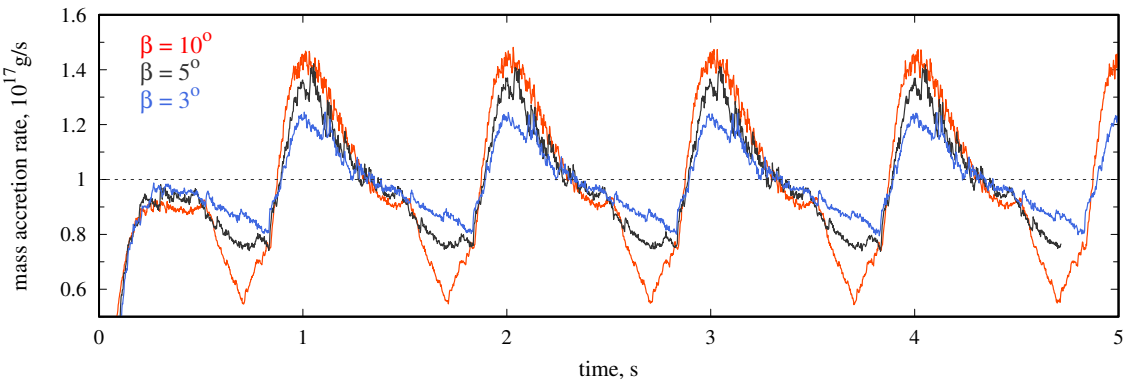

Figure 6. *Mass accretion rate onto an NS surface given as a function of time in units of mass accretion rate at the inner disc radius. Different curves are calculated for different angles between the rotation axis and normal to the disc plane.* $P_{\rm spin} = 1\,\mathrm{s}$, $\alpha = 0.3\,\mathrm{rad}$, *and* $\dot{M}_{\rm disk} = 10^{17}\,\mathrm{g\,s^{-1}}$ *for all rotators modeled in this figure.*

normalized by the mass accretion rate at the inner disc radius. The curves correspond to different angles, α, between the NS rotational axis and the normal to the accretion disc plane.

Our simulations reveal that the amplitude of the mass accretion rate variability depends significantly on this angle. Even for small misalignment angles, such as $\beta \sim 3°$, the variability amplitude remains substantial, reaching levels of 10–20%. Larger angles result in greater variability, as the misalignment increases the deviation of the flow from a symmetric distribution around the magnetic poles.

These results suggest that the angular misalignment introduces a pronounced modulation in the mass accretion process. The variability in the accretion rate could influence the emission

properties of XRPs, potentially contributing to the asymmetric features often observed in their pulse profiles. Together with the results from the previous figure, this analysis highlights the importance of both the NS spin period and the angular misalignment in determining the characteristics of mass accretion rate variability at the NS surface.

Magnetic obliquity - that is, the misalignment of magnetic dipole and rotational axes - is a key parameter in these simulations, and a non-zero magnetic obliquity can lead to time-dependent mass accretion rates and hence much more significant asymmetry in the XRP pulse profile. However, fully investigating this parameter will require more extensive simulations. The faculty advisor of this paper is currently working on a dedicated paper investigating this parameter.

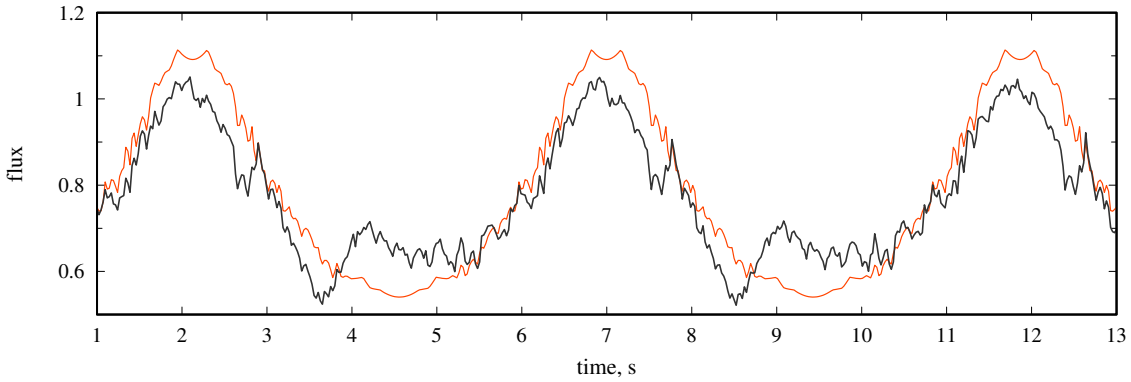

Figure 7. *Modeled X-ray energy flux from XRP, where the rotation of an NS is aligned (red curve) and misaligned (black curve, $\alpha = 0.3$ rad) with the dipole axis. One can see that misalignment of NS rotation results in asymmetry of the expected pulse profile [5]. Parameters: $P_{\rm spin} = 5$ s, $M = 1.4\,M_\odot$, $R = 10^6$ cm, $\beta = 0.2$ rad.*

Figure 7 shows the modeled photonic flux from an XRP for two scenarios: a neutron star (NS) with the rotational axis aligned with the dipole axis (red curve) and a misaligned NS (black curve). The results clearly demonstrate that the misalignment between the NS rotation axis, the accretion disc plane, and the magnetic moment introduces asymmetry into the expected pulse profile.

When the rotation and dipole axes are aligned, the energy flux remains symmetric, consistent with the uniform accretion of material onto the magnetic poles. However, in the misaligned case, the variability in the mass accretion rate at the NS surface induced by the misalignment leads to variable luminosity at the poles, and hence noticeable asymmetry in the pulse profile. The shape and amplitude of this asymmetry depend on the degree of misalignment, as well as the interplay of rotational modulation and the geometry of the emission region.

This asymmetry in the pulse profile provides a potential explanation for the irregularities often observed in the pulse shapes of XRPs. It underscores the importance of accounting for geometric factors, such as the misalignment of the NS rotation axis, in modeling the X-ray emission from accreting neutron stars.

5. Summary. In this study, we investigated the accretion process in XRPs with misaligned dipole, rotational, and disc plane axes. Our analysis is restricted to cases where the NS magnetic field is dominated by a dipole component, and the magnetic dipole itself remains undisturbed by the accretion process. A full solution taking into consideration the distortion of magnetic fields due to large magnetospheric currents will require a solution of the reduced magnetohydrodynamic (RMHD) equations, which is beyond the scope of this publication. Furthermore, recent evidence [4] demonstrates that magnetospheres of some XRPs can possess a multipole component [3, 13, 7], which would significantly complicate accretion dynamics calculations and would significantly influence the observed patterns.

We numerically calculated the motion of particles along the magnetic field lines, accounting for gravitational and centrifugal forces, with radiative forces also being estimated. Through these simulations, we calculated the mass accretion rate at the NS surface as a function of time. Our results indicate that the misalignment between the NS rotation axis and the accretion disc plane leads to a variable mass accretion rate onto the NS surface. This variability exhibits periodic behavior with the NS spin period, as shown in Figure 5 and Figure 6. The amplitude of the variability depends on the NS spin period and the angles between rotational, dipole, and disc plane axes. Specifically, we find that the amplitude of the variations in the mass accretion rate decreases for longer spin periods and remains significant (10 % to 20 %) even for small angles of misalignment ($\sim 3^\circ$).

This variability also leads to periodic asymmetry in the observed X-ray flux of the XRP, as shown in Figure 7. Hence, we propose that such periodic variations in the mass accretion rate on the NS surface caused by misaligned dipole, rotational, and accretion disc plane axes could lead to the asymmetric pulse profiles commonly observed in many XRPs (see Figure 7).

6. Appendix. We start by considering the various frames of reference associated with the XRP. These are

1. The disk frame (denoted by subscript d);
2. The rotational frame (denoted by subscript ω);
3. The magnetic field frame (denoted by subscript B).

We then proceed by considering the inclination between them. We assume that the frames share a common origin, and at $t = 0$, $\mathbf{x_d} = \mathbf{x_\omega} = \mathbf{x}_\mathrm{B}$, so all the y- and z- axes differ from each other by at most an angle.

We define the angle β as the angle between $\mathbf{z_d}$ and $\mathbf{z_\omega}$, and the angle α (unrelated to the angle α_γ that determines the photon trajectory) as the angle between $\mathbf{z_\omega}$ and $\mathbf{z}_\mathrm{B}$. We can use these two angles to write the transformations between the frames as rotation matrices:

$$M_{d\omega} = \begin{bmatrix} 1 & 0 & 0 \\ 0 & \cos\beta & -\sin\beta \\ 0 & \sin\beta & \cos\beta \end{bmatrix} \tag{6.1}$$

$$M_{\omega\mathrm{B}} = \begin{bmatrix} 1 & 0 & 0 \\ 0 & \sin\alpha & -\cos\alpha \\ 0 & \cos\alpha & \sin\alpha \end{bmatrix} \tag{6.2}$$

Additionally, we model the rotation of the ω frame by restricting the angular velocity of the XRP $\boldsymbol{\omega}$ to the z_ω-axis. The rotation of the coordinate system is thus given by:

$$M_w = \begin{bmatrix} \cos\omega t & -\sin\omega t & 0 \\ \sin\omega t & \cos\omega t & 0 \\ 0 & 0 & 1 \end{bmatrix} \tag{6.3}$$

where ω is the angular frequency of the XRP rotation. Applying the transformations in sequence, we have:

$$M_{dB} = M_{d\omega} M_w M_{\omega\mathrm{B}}$$

Now, we consider the accretion disk plane. The normal $\mathbf{n}$ to this plane is given by $(0, 0, 1)$ in $(x_\mathrm{B}, y_\mathrm{B}, z_\mathrm{B})$ coordinates. Applying the matrix $M_{d\mathrm{B}}$ to this vector, we see that $\mathbf{n}$ is given by

$$\mathbf{n} = \begin{bmatrix} \sin\beta\sin\omega t \\ -(\cos\beta\sin\alpha + \cos\alpha\sin\beta\cos\omega t) \\ \cos\beta\cos\alpha - \sin\beta\sin\alpha\cos\omega t \end{bmatrix} \tag{6.4}$$

in B-coordinates. Given $\mathbf{n}$, we then apply Eqn. (2.7) to the values from this plane to find the slope angle for any given φ, which gives us the complete, time-varying and accurate formula for the latitude of the accretion disk as a function of rotational phase and azimuthal angle.

Acknowledgments. The author acknowledge the Cambridge Center for International Research for their help in facilitating coordination and collaboration.

The first author also thanks D r. Alexander Mushtukov, the faculty advisor, for his advice, guidance, and support over the course of this project.

REFERENCES

[1] C. Flexer and A. A. Mushtukov, *Coupling of radiation and magnetospheric accretion flow in ulx pulsars: radiation pressure and photon escape time*, Monthly Notices of the Royal Astronomical Society, 529 (2024), pp. 1571–1578, https://doi.org/10.1093/mnras/stae653, https://doi.org/10.1093/mnras/stae653, https://arxiv.org/abs/https://academic.oup.com/mnras/article-pdf/529/2/1571/56989982/stae653.pdf.

[2] J. Frank, A. King, and D. J. Raine, *Accretion Power in Astrophysics: Third Edition*, 2002.

[3] G. L. Israel, A. Belfiore, L. Stella, P. Esposito, P. Casella, A. De Luca, M. Marelli, A. Papitto, M. Perri, S. Puccetti, G. A. R. Castillo, D. Salvetti, A. Tiengo, L. Zampieri, D. D'Agostino, J. Greiner, F. Haberl, G. Novara, R. Salvaterra, R. Turolla, M. Watson, J. Wilms, and A. Wolter, *An accreting pulsar with extreme properties drives an ultraluminous x-ray source in NGC 5907*, Science, 355 (2017), pp. 817–819, https://doi.org/10.1126/science.aai8635, https://arxiv.org/abs/1609.07375.

[4] C. Kalapotharakos, Z. Wadiasingh, A. K. Harding, and D. Kazanas, *The Multipolar Magnetic Field of the Millisecond Pulsar PSR J0030+0451*, The Astrophysical Journal, 907 (2021), p. 63, https://doi.org/10.3847/1538-4357/abcec0, https://iopscience.iop.org/article/10.3847/1538-4357/abcec0 (accessed 2024-12-05).

[5] U. Kraus, *Hollow Accretion Columns on Neutron Stars and the Effects of Gravitational Light Bending*, , 563 (2001), pp. 289–300, https://doi.org/10.1086/323791.

[6] V. M. Lipunov and N. I. Shakura, *On the nature of binary-system X-ray pulsars*, Soviet Astronomy Letters, 2 (1976), pp. 133–135, https://ui.adsabs.harvard.edu/abs/1976SvAL....2..133L (accessed 2024-11-22). ADS Bibcode: 1976SvAL....2..133L.

[7] J. Mönkkönen, S. S. Tsygankov, A. A. Mushtukov, V. Doroshenko, V. F. Suleimanov, and J. Poutanen, *Constraints on the magnetic field structure in accreting compact objects from aperiodic variability*, , 515 (2022), pp. 571–580, https://doi.org/10.1093/mnras/stac1828, https://arxiv.org/abs/2206.01502.

[8] A. Mushtukov and S. Tsygankov, *Accreting strongly magnetised neutron stars: X-ray Pulsars*, Apr. 2023, https://doi.org/10.48550/arXiv.2204.14185, http://arxiv.org/abs/2204.14185 (accessed 2024-11-22). arXiv:2204.14185 [astro-ph].

[9] A. A. Mushtukov, A. Ingram, V. F. Suleimanov, N. DiLullo, M. Middleton, S. S. Tsygankov, M. van der Klis, and S. Portegies Zwart, *Magnetospheric flows in X-ray pulsars - I. Instability at super-Eddington regime of accretion*, , 530 (2024), pp. 730–742, https://doi.org/10.1093/mnras/stae781, https://arxiv.org/abs/2402.12965.

[10] M. M. Romanova, G. V. Ustyugova, A. V. Koldoba, and R. V. E. Lovelace, *Three-dimensional simulations of disk accretion to an inclined dipole. ii. hot spots and variability*, The Astrophysical Journal, 610 (2004), p. 920, https://doi.org/10.1086/421867, https://dx.doi.org/10.1086/421867.

[11] M. M. Romanova, G. V. Ustyugova, A. V. Koldoba, J. V. Wick, and R. V. E. Lovelace, *Three-dimensional simulations of disk accretion to an inclined dipole. i. magnetospheric flows at different* , The Astrophysical Journal, 595 (2003), p. 1009, https://doi.org/10.1086/377514, https://dx.doi.org/10.1086/377514.

[12] O. Toropina, M. Romanova, and R. Lovelace, *Accretion to a Magnetized Neutron Star in the "Propeller" Regime*, in 13th Young Scientists' Conference on Astronomy and Space Physics, A. Golovin, G. Ivashchenko, and A. Simon, eds., June 2006, p. 107, https://doi.org/10.48550/arXiv.astro-ph/0607189, https://arxiv.org/abs/astro-ph/0607189.

[13] S. S. Tsygankov, V. Doroshenko, A. A. Lutovinov, A. A. Mushtukov, and J. Poutanen, *SMC X-3: the closest ultraluminous X-ray source powered by a neutron star with non-dipole magnetic field*, , 605 (2017), A39, p. A39, https://doi.org/10.1051/0004-6361/201730553, https://arxiv.org/abs/1702.00966.